HYDROLYTIC PROCESSING OF RICE HUSKS IN AQUEOUS MEDIA: A KINETIC ASSESSMENT

Carlos VILA[1], Gil GARROTE[2], Herminia DOMÍNGUEZ[3] and Juan Carlos PARAJÓ[4,*]

Department of Chemical Engineering, University of Vigo, Polytechnical Building, As Lagoas, 32004 Ourense, Spain; e-mail: [1] cvila@uvigo.es, [2] gil@uvigo.es, [3] herminia@uvigo.es, [4] jcparajo@uvigo.es

Received November 26, 2001
Accepted February 25, 2002

The kinetics of hemicellulose decomposition in the non-isothermal rice husk autohydrolysis was experimentally assessed. Experimental data on the time course of the concentrations of hemicellulosic polymers (xylan, araban and acetyl groups) and their autohydrolysis products (including sugar oligomers, monosaccharides, furfural and acetic acid) were fitted to several kinetic models based on multiple pseudohomogeneous first-order reactions. Sugar oligomers were the major reaction products. The hydrolytic conversion of xylan, araban and acetyl groups was well interpreted by kinetic models based on consecutive and parallel reactions.
Keywords: Acetyl groups; Araban; Autohydrolysis; Rice husks; Kinetics; Modelling; Oligomers; Xylan.

Chemical utilisation of lignocellulosic materials can be carried out according to the "biomass refining" philosophy[1]: the main components of feedstocks (cellulose, hemicelluloses and lignin) can be fractionated by sequential treatment to give separate streams that may be used for different product applications. A possible process for the full utilisation of biomass may start with a hydrolytic stage (carried out in aqueous media with possible addition of acids) in which the hemicellulosic fraction is solubilised, while both cellulose and lignin remain in the solid phase with little alteration. The liquors from the treatment (containing hemicellulose-degradation products such as sugar oligomers, monosaccharides, acetic acid, furfural and hydroxymethylfurfural) are easily separated from the solid phase, which can be subjected to further processing (for example, organosolv pulping) to achieve the separation of cellulose and lignin.

The hydrolytic degradation of hemicelluloses goes through the acid-catalysed cleavage of heterocyclic ether bonds linking monosaccharide units. For this purpose, the reaction can be catalysed either by externally added mineral acids ("prehydrolysis" stage) or by hydronium ions gener-

ated *in situ* (by water ionisation in the first reaction stages and by autoionisation of acetic acid generated from acetyl groups in further reaction stages). This second approach (here denoted autohydrolysis) shows comparative advantages over prehydrolysis: water and feedstock are the only reagents, the reaction is carried out under mild pH conditions (limiting the degradation reactions), no neutralisation sludges are generated, and both cellulose and lignin are susceptible to further separation reactions (cellulose is not significantly degraded, and a part of the α and β aryl ether bonds of lignin are cleaved, making the phenolic fraction soluble in organic solvents or dilute alkali solutions).

The effect caused by autohydrolysis depends on the lignocellulosic substrate employed. The term "hemicelluloses" refers to heteropolymers made up of sugars (such as xylose, arabinose, mannose, galactose, glucose or rhamnose), a part of which can be substituted (for example, with acetyl groups or uronic units). In the case of lignocellulosic materials of agricultural origin, the main monomeric sugars acting as structural units of hemicelluloses are xylose and arabinose, and the corresponding polymers (xylan and araban) can be partly acetylated.

During the autohydrolysis reactions, the hemicellulosic polysaccharides are degraded mostly to sugar oligomers and sugars. Under harsh reaction conditions, both arabinose and xylose can be dehydrated to furfural, which can undergo decomposition reactions. On the other hand, acetyl groups are splitted off in the autohydrolysis medium, leading to the formation of acetic acid[2,3].

Under the reaction conditions usually employed in the autohydrolysis treatment, sugar oligomers (mainly xylooligomers) are major reaction products[3,5–7], in concentrations which can account for more than 50% of the initial hemicelluloses[8–11]. Xylooligomers are currently used as new sweeteners or food additives[12]. Health applications of indigestible oligosaccharides have been reported in this field[13,14]. Improvements in gastrointestinal health of rats caused by a xylooligomer-containing diet have been reported[15]. Regarding the human health, xylooligomers selectively enhance the growth of Bifidobacteria, thus promoting a favourable intestinal environment[15–17]. Alternatively, the xylooligomer solutions produced in autohydrolysis can be converted into xylose solutions by acid-catalysed posthydrolysis[18]. The manufacture of xylose solutions by performing successive stages of autohydrolysis and posthydolysis shows advantages for further biotechnological conversion over the conventional single-stage prehydrolysis, because the milder reaction conditions result in de-

creased contents of reaction byproducts causing inhibition of the microbial metabolism.

This work deals with the kinetic modelling of rice husk autohydrolysis under non-isothermal conditions, with the objective of providing a sound basis for the kinetic interpretation of a heterogeneous system where simultaneous reactions (leading to several products of commercial interest) occur. Experimental data concerning the time course of hemicellulose components (xylan, araban and acetyl groups) and their reaction products (sugar oligomers, monosaccharides, furfural and acetic acid) were fitted to several kinetic models based on multiple pseudohomogeneous first-order reactions in order to assess the experimental findings.

MATERIALS AND METHODS

Raw Material

Rice husk samples from a local factory were air-dried, homogenised in a single lot to avoid differences in composition among aliquots, and stored.

Analysis of Raw Material

Aliquots from the above homogenised lot were subjected to moisture determination and to quantitative acid hydrolysis with 72% sulfuric acid following standard methods[19]. The solid residue after hydrolysis was considered as Klason lignin. The monosaccharides and acetic acid contained in hydrolysates were determined by HPLC as reported elsewhere[20].

Hydrothermal Processing of Samples

Rice husks and water were mixed and reacted in a Parr reactor fitted with double six-blade turbine impellers. The vessel was heated with external fabric mantles, and cooled with an internal stainless steel loop. Temperature was monitored using an inner thermocouple, and controlled by a PID module. Time zero was taken when the reaction temperature reached 50 °C. The reaction media were heated for the predetermined time, and then cooled. After achieving normal pressure, the reactor was opened and samples of the suspensions were withdrawn.

Analysis of Liquors from Hydrothermal Treatments

At the end of treatment, the solid residue was recovered by filtration. A sample of the liquors was filtered through 0.45-μm membranes and used for direct HPLC determination of glucose, xylose, arabinose, furfural, and acetic acid. A second sample of liquors was subjected to quantitative posthydrolysis (with 4% sulfuric acid at 121 °C for 60 min) before duplicate HPLC analysis. The increase in the concentrations of monosaccharides and acetic acid caused by posthydrolysis provided a measure of the oligomer concentration and their degree of substitution with acetyl groups[9].

Fitting of Data

Empirical equations (selected from built-in functions of the TableCurve software, Jandel Scientific, U.S.A.) were used to fit the temperature profiles (which were measured for each experiment and averaged before fitting). The empirical equations obtained were used in the numerical solving of the differential equations involved in the models. The sets of differential equations corresponding to the various kinetic models were solved by the fourth order Runge–Kutta method. A commercial optimisation routine utilising the Newton method was used to calculate the pre-exponential factors and the activation energies by minimising the sum of the squares of deviations between experimental and calculated data according to the philosophy reported elsewhere[10,11].

RESULTS AND DISCUSSION

Raw Material Composition

The rice husk lot employed in this work was assayed for its contents of cellulose, hemicelluloses (including xylan, araban and acetyl groups), lignin, ashes and others (by difference). The average results obtained after four replicate determinations and the standard deviations of data are presented in Table I.

Kinetics of Hydrolytic Degradation of Polysaccharides in Lignocellulosic Materials

The hydrolytic degradation of polysaccharides (including cellulose and hemicelluloses) in aqueous or acid-containing media (hydrolysis, pre-

TABLE I
Composition of rice husk (as the average of four replicate determinations)

Fraction	Weight, % (dry basis)	Standard deviation
Cellulose	36.7	0.74
Xylan	15.6	0.12
Araban	1.68	0.00
Acetyl groups	1.62	0.14
Klason lignin	21.3	0.08
Ash	14.3	0.09
Others (by difference)	8.80	–

hydrolysis or autohydrolysis reactions) follow the same kinetic principles because all of them are based on the hydronium-catalysed breakdown of glycosidic bonds.

In the case of hemicellulose hydrolysis, there is experimental evidence that in some cases, the reaction follows a two-stage kinetics: the conversion of 60–90% of the substrate proceeds faster than the residual fraction[21]. Because of this, the suggestion of Kobayashi and Sakai[22], who assumed the presence of two hemicellulose fractions with different susceptibility to hydrolysis, has been followed by some authors. The two-fraction hypothesis can be justified by reasons such as the existence of mass and heat transfer limitations in partially converted substrates, accessibility problems, variation in particle size and available surface area in the hydrolytic process and differences in reactivity caused by a different composition or a different substitution pattern of the unreacted substrate[2,21,23–25]. The fraction of hemicelluloses susceptible to hydrolysis (denoted "susceptible fraction", α) depends on both the lignocellulose feedstock and the reaction conditions under which the reaction was performed[21].

In the mathematical interpretation of the oligomer generation during the autohydrolysis of lignocellulose, it must be considered that the breakdown of a given bond can lead to different reaction products (monosaccharides or oligosaccharides) depending on the position of the cleaved bond in the polymer chain. When hemicelluloses have been consumed to a significant extent, oligomers are the most abundant reactive species in the medium. Considering that the degree of polymerisation (DP) of hemicellulosic polysaccharides is usually in the range 50–300, first reaction stages lead mainly to oligomers. Further reaction results in increased concentrations of low-DP oligomers, and also in increased sugar formation[8]. Operating with high catalyst concentrations (for example, in prehydrolysis reactions), oligomers are decomposed in a fast reaction[26], reaching limited concentrations, and their formation can be neglected in an overall mechanism describing the polymer degradation[27]. This simplification has no influence on further economic or design calculations[28].

Reported studies on hydrolytic conversion of polysaccharides (including cellulose and hemicelluloses) are based on pseudohomogeneous kinetics, where the kinetic parameters follow an Arrhenius-type dependence on temperature. The pioneering study of acid hydrolysis of cellulose reported by Saeman[29] proposed the Model 1 in Fig. 1. Further studies included the participation of two cellulose fractions of different reactivity[30], the participation of oligomers as reaction intermediates[31] (see Model 2 in Fig. 1), the possibility of glucose decomposition, with formation of compounds such as

Model 1 (Saeman, 1945)

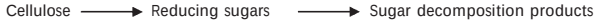

Model 2 (Abatzoglou *et al.*, 1986)

Model 3 (McKibbins *et al.*, 1962)

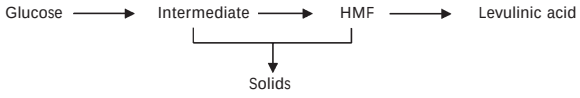

Model 4 (Mok, Antal and Varhegyi, 1992)

Model 5 (Conner *et al.*, 1985; Harris *et al.*, 1985)

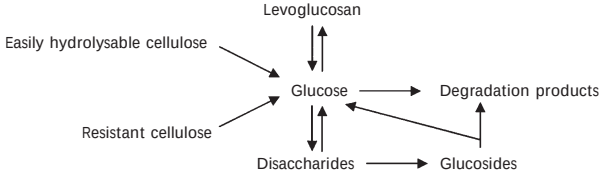

Model 6 (Bouchard *et al.*, 1989)

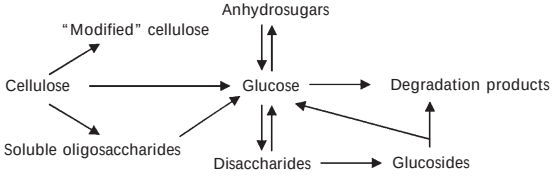

Model 7 (Madeleine, Bouvier and Gelus, 1990)

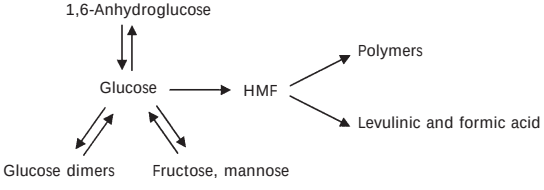

FIG. 1
Models reported for the acid hydrolysis of cellulose

(hydroxymethyl)furfural (HMF) or levulinic acid[32] (see Model 3 in Fig. 1), the generation of non-hydrolysable compounds[33] (see Model 4 in Fig. 1) or the participation of other reactions in the overall mechanism[34–36] (*e.g.* Models 5–7 in Fig. 1).

Several studies applied related ideas to the hydrolysis of hemicelluloses in the presence of added acid (prehydrolysis reaction). In these cases, hemicelluloses were considered to be xylan, a xylose homopolymer. The modelling of wood prehydrolysis under mild conditions has been carried out considering that xylose is generated from two xylan fractions with different susceptibility to hydrolysis[37] (see Model 1 in Fig. 2). Under harsher reaction conditions, the decomposition of xylose must be considered, according to Model 2 in Fig. 2 (ref.[38]). The possibility of furfural generation from xylose and furfural decomposition is considered in Models 3 (ref.[39]) and 4 (ref.[27]) in Fig. 2. In some studies, the generation of xylooligomers from xylan has been included in the overall reaction scheme. This situation is considered in Models 5 (ref.[40]) and 6 (ref.[23]) in Fig. 2.

In comparison with prehydrolysis, the kinetic modelling of autohydrolysis is more complicated owing to the lower availability of catalyst, which results in increased importance of oligomer generation. Of the scarce research carried out in this field, the fact that the proportion of low-DP oligomers (susceptible to be hydrolysed to monosaccharides with high probability) increases with the extent of the reaction was interpreted[8] assuming a time-dependent kinetic parameter for the conversion of xylooligomers into xylose (see Model 1 in Fig. 3). The equation describing such a dependence was:

$$k_O = k_{O\,max}\,[1 - \exp(-\beta\tau)]\,, \qquad (1)$$

where k_O is the kinetic coefficient, and the parameters $k_{O\,max}$ and β are calculated from experimental results. This procedure allowed a better reproduction of data than the case where k_O was not time-dependent[23] (Model 6, Fig. 2). Garrote, Domínguez and Parajó[9,10] proposed Models 2 and 3 in Fig. 3, in which the progressive reduction in molecular weight observed during the autohydrolysis was simplified to two consecutive reactions, the first one leading to high-DP oligomers from xylan, and the second one leading to low-DP oligomers from high-DP oligomers. In the case of Model 2, the raw material (Eucalyptus wood) contains an unreactive xylan fraction under the reaction conditions considered, and furfural was not significantly decomposed. In the case of Model 3, developed for corncobs,

Model 1 (Parajó *et al.*, 1993)

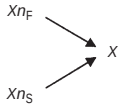

Model 2 (Kim and Lee, 1987)

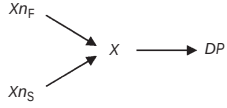

Model 3 (Brennan, Hoagland and Schell, 1986)

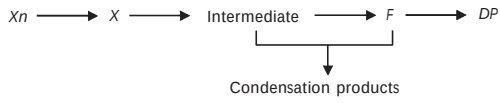

Model 4 (Abatzoglou *et al.*, 1990)

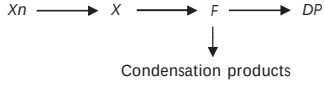

Model 5 (Mehlberg and Tsao, 1979)

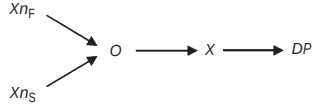

Model 6 (Conner, 1984)

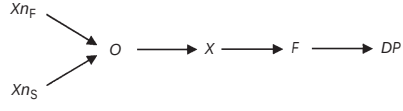

FIG. 2

Models reported for the prehydrolysis of hemicelluloses. Nomenclature: Xn_F, fast-reacting xylan; Xn_S, slow-reacting xylan; *X*, xylose; *DP*, degradation products; *Xn*, xylan; *F*, furfural; *O*, oligomers

the model includes direct furfural generation from low-DP oligomers, as well as furfural consumption by parasitic reactions.

Kinetic Modelling of Xylan Autohydrolysis

Based on material balances concerning xylan, oligomers, xylose and furfural, two "developed" models (Models 1 and 2, Fig. 4) were selected for preliminary data analysis. The first one is a simplification of Model 6 in Fig. 2, in which the step of furfural decomposition was omitted, and the other is closely related to Model 3 in Fig. 3, where furfural was generated from both low-DP xylooligomers and xylose. These "developed" models were assayed together with six other additional models resulting from simplifications of them. Table II lists the hypotheses considered in the formulation of the set of kinetic models (denoted A to H). The several approachs considered the following possibilities: xylan can be made up of one or two fractions susceptible to hydrolysis (whose relative proportions are given by the parameter α); in the case with models with a single oligomer fraction, the kinetic coefficient governing the xylooligomer fraction can be time-dependent (through the equation proposed by Conner and Lorenz[10]) whereas

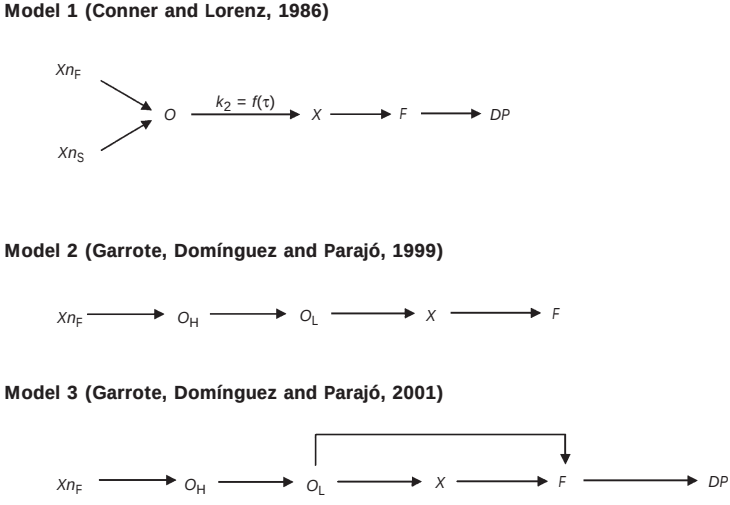

FIG. 3

Models reported for the autohydrolysis of hemicelluloses. Nomenclature: Xn_F, fast-reacting xylan; Xn_S, slow-reacting xylan; *X*, xylose; *DP*, degradation products; *Xn*, xylan; *F*, furfural; *O*, oligomers; O_H, high-molecular weight oligomers; O_L, low-molecular weight oligomers

(in the models dealing with two oligomer fractions) furfural can be produced from low-DP oligomers and/or xylose. The temperature dependence of the kinetic parameters included in Models B and D was established using the equation

TABLE II
Specifications of the kinetic models employed in this work

Model	Starting form	Assumption
A	model 1 in Fig. 4	$k_2 \neq f(\tau)$
B	model 1 in Fig. 4	$k_2 = f(\tau) = k_{2\max}[1 - \exp(-\beta\tau)]$
C	model 1 in Fig. 4	$k_{1S} = 0$ $k_2 \neq f(\tau)$
D	model 1 in Fig. 4	$k_{1S} = 0$ $k_2 = f(\tau) = k_{2\max}[1 - \exp(-\beta\tau)]$
E	model 2 in Fig. 4	–
F	model 2 in Fig. 4	$k_4 = 0$
G	model 2 in Fig. 4	$k_{1S} = 0$
H	model 2 in Fig. 4	$k_{1S} = 0$ $k_4 = 0$

Model 1, employed in this work

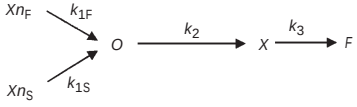

Model 2, employed in this work

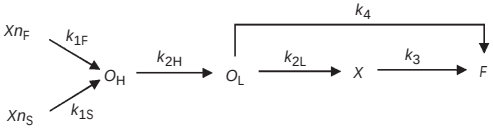

FIG. 4
Models employed in this work for the modelling of rice husk autohydrolysis. Nomenclature as in Fig. 3

$$k_2 = k_{2\,\max} \exp\left(-\frac{E_{a2}}{RT}\right)[1-\exp(-\beta\tau)]\,. \qquad (2)$$

Assuming that all the reactions participating in Model 1 in Fig. 4 are of first order and present an Arrhenius-type dependence on temperature, the whole xylan degradation is described by the following set of differential equations:

$$\frac{\mathrm{d}Xn_F}{\mathrm{d}\tau} = -k_{0F} \exp\left[\frac{-E_{aF}}{RT(\tau)}\right] Xn_F \qquad (3)$$

$$\frac{\mathrm{d}Xn_S}{\mathrm{d}\tau} = -k_{0S} \exp\left[\frac{-E_{aS}}{RT(\tau)}\right] Xn_S \qquad (4)$$

$$\frac{\mathrm{d}O}{\mathrm{d}\tau} = k_{0F} \exp\left[\frac{-E_{aF}}{RT(\tau)}\right] Xn_F + k_{0S} \exp\left[\frac{-E_{aS}}{RT(\tau)}\right] Xn_S -$$

$$k_{2\,\max} \exp\left[\frac{-E_{a2}}{RT(\tau)}\right][1-\exp(-\beta\tau)]O \qquad (5)$$

$$\frac{\mathrm{d}X}{\mathrm{d}\tau} = k_{2\,\max} \exp\left[\frac{-E_{a2}}{RT(\tau)}\right][1-\exp(-\beta\tau)]O - k_{03} \exp\left[\frac{-E_{a3}}{RT(\tau)}\right] X\,, \qquad (6)$$

where $T(\tau)$ is the temperature (in K) achieved at the considered reaction time τ following the temperature profile shown in Fig. 5, Xn_F is the percentage of fast-reacting xylan remaining in the substrate at the considered reaction time, Xn_S is the percentage of slow-reacting xylan remaining in the substrate at the considered reaction time, O is the percentage of initial xylan converted into xylooligomers, X is the percentage of initial xylan converted into xylose. The values of variable F (percentage of initial xylan converted into furfural) are calculated by a material balance to the xylan-derived compounds.

In a similar approach, the equations describing the xylan degradation according to Model 2 in Fig. 4 are:

$$\frac{\mathrm{d}Xn_{\mathrm{F}}}{\mathrm{d}\tau} = -k_{0\mathrm{F}} \exp\left[\frac{-E_{\mathrm{aF}}}{RT(\tau)}\right] Xn_{\mathrm{F}} \tag{7}$$

$$\frac{\mathrm{d}Xn_{\mathrm{S}}}{\mathrm{d}\tau} = -k_{0\mathrm{S}} \exp\left[\frac{-E_{\mathrm{aS}}}{RT(\tau)}\right] Xn_{\mathrm{S}} \tag{8}$$

$$\frac{\mathrm{d}O_{\mathrm{H}}}{\mathrm{d}\tau} = k_{0\mathrm{F}} \exp\left[\frac{-E_{\mathrm{aF}}}{RT(\tau)}\right] Xn_{\mathrm{F}} + k_{0\mathrm{S}} \exp\left[\frac{-E_{\mathrm{aS}}}{RT(\tau)}\right] Xn_{\mathrm{S}} - k_{02\,\mathrm{H}} \exp\left[\frac{-E_{\mathrm{a}2\,\mathrm{H}}}{RT(\tau)}\right] O_{\mathrm{H}} \tag{9}$$

$$\frac{\mathrm{d}O_{\mathrm{L}}}{\mathrm{d}\tau} = k_{02\,\mathrm{H}} \exp\left[\frac{-E_{\mathrm{a2H}}}{RT(\tau)}\right] O_{\mathrm{H}} - \left\{k_{02\,\mathrm{L}} \exp\left[\frac{-E_{\mathrm{a2L}}}{RT(\tau)}\right] + k_{04} \exp\left[\frac{-E_{\mathrm{a4}}}{RT(\tau)}\right]\right\} O_{\mathrm{L}} \tag{10}$$

$$\frac{\mathrm{d}X}{\mathrm{d}\tau} = k_{02\,\mathrm{L}} \exp\left[\frac{-E_{\mathrm{a}2\,\mathrm{L}}}{RT(\tau)}\right] O_{\mathrm{L}} - k_{03} \exp\left[\frac{-E_{\mathrm{a3}}}{RT(\tau)}\right] X\,, \tag{11}$$

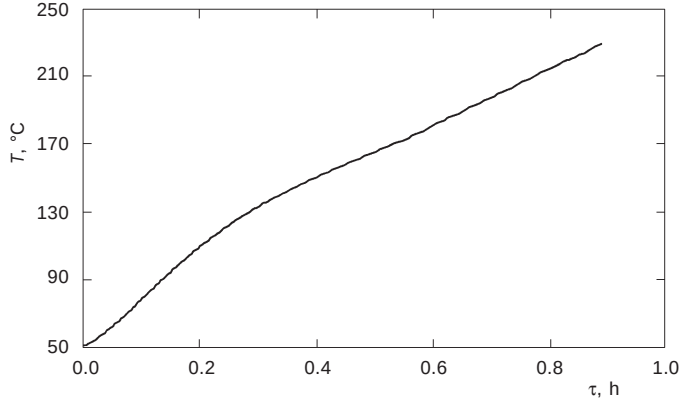

Fig. 5
Heating profile employed in this study

where O_H is the percentage of initial xylan converted into high-molecular weight xylooligomers and O_L is the percentage of initial xylan converted into low-molecular weight xylooligomers.

In Eqs (*3*)–(*11*), k_{0F}, k_{0S}, k_{02H}, k_{02L}, k_{03}, and k_{04} denote the pre-exponential factors, E_{aF}, E_{aS}, E_{a2H} E_{a2L}, E_{a3}, and E_{a4} denote the activation energies and $k_{2\,max}$ and β give the time dependence of the kinetic coefficient governing the xylooligomer hydrolysis to xylose.

The numerical integration of the above sets of equations can be carried out considering the following equations

$$Xn = Xn_F + Xn_S \tag{12}$$

$$\alpha = \frac{Xn_{F0}}{Xn_0} \tag{13}$$

and for Model 2 in Fig. 4,

$$O = O_H + O_L\,, \tag{14}$$

where Xn is the percentage of total xylan remaining in the substrate at the considered reaction time and α is the weight fraction of fast-reacting xylan in the untreated substrate (measured as the ratio between initial fast-reacting xylan Xn_{F0} and initial xylan Xn_0). For calculation purposes, α was considered to be independent of temperature under the reaction conditions tested.

As the experimental data do not allow a distinction between high- and low-DP xylooligomers, the values of the kinetic coefficients k_{2H} and k_{2L} in Model 2 in Fig. 4 have been calculated by minimisation of the sum of the squared deviations of the term (O_H + O_L) from the experimental values determined for the total xylooligomer concentrations.

The equations describing Model 1 in Fig. 4 (Eqs (*3*)–(*6*), (*12*) and (*13*)) and Model 2 in Fig. 4 (Eqs (*7*)–(*14*)) have been solved numerically using the fourth order Runge–Kutta method coupled with an optimisation algorithm, as described in the Materials and Methods section.

For each series of experimental data, the mean relative quadratic deviation (δ, expressed as %) was calculated as follows:

$$\delta = 100\sqrt{\frac{1}{n}\sum_{i=1}^{i=n}\left(\frac{x_{exp}}{x_{calc}} - 1\right)_i^2} \quad , \qquad (15)$$

where x_{exp} and x_{calc} denote the experimental and calculated results for the considered variable, and n is the number of measurements.

The values obtained for the regression parameters participating in the models are shown in Tables III and IV, whereas Figs 6 and 7 allow a comparison between experimental and calculated results. From the results calculated for various models, it can be seen that the assumption of two

TABLE III
Values calculated for the kinetic parameters participating in models A, C, E, F, G, and H in Table II (E_{ai} in kJ mol^{-1}; k_{0i} in h^{-1})

Hydrolysis substrate	Kinetic parameters	Model					
		A[a]	C[a]	E	F	G	H
Xylan	$\ln k_{0F}$	50.2	50.2	50.2	50.2	50.2	50.2
	E_{aF}	188	188	188	188	188	188
	$\ln k_{0S}$	19.9	–	19.9	19.9	–	–
	E_{aS}	125	–	125	125	–	–
	α	0.916	0.916	0.916	0.916	0.916	0.916
	δ	8.49	8.49	8.49	8.49	8.49	8.49
Xylooligomers	$\ln k_{02H}$	64.8	64.8	50.4	50.4	50.4	50.4
	E_{a2H}	257	257	198	198	198	198
	$\ln k_{02L}$	–	–	57.5	57.5	57.5	57.5
	E_{a2L}	–	–	216	216	216	216
	$\ln k_{04}$	–	–	35.3	–	42.9	–
	E_{a4}	–	–	166	–	166	–
	δ	15.77	15.77	15.91	15.89	15.90	15.90
Xylose	$\ln k_{03}$	45.7	45.7	48.4	44.2	44.1	44.2
	E_{a3}	168	168	185	161	161	161
	δ	14.51	20.95	18.30	26.79	21.30	34.19

[a] Models with a single xylooligomer fraction, where k_{2H} stands for k_2.

reacting xylan fractions does not significantly improve the accuracy of the predictions. Hence, the simplest approach (the xylooligomers are generated from a single xylan fraction, or $k_{1S} = 0$), which involves a minimum number of regression parameters, was preferred. On the other hand, the assumption of time-dependent coefficients (Models B and D in Table II) does not improve the data interpretation. The models involving two oligosaccharide fractions (Models E–H in Table II) provided a better reproduction of experimental data than those involving a single oligosaccharide fraction (Models C and D in Table II).

Based on the above ideas, Model H in Table II was the simplest one providing an adequate description of the experimental findings. The corresponding reaction scheme is as follows.

$$Xn_F \xrightarrow{k_1} O_H \xrightarrow{k_2} O_L \xrightarrow{k_3} X \xrightarrow{k_4} F$$

TABLE IV
Values calculated for the kinetic parameters participating in models B and D in Table II (E_{ai} in kJ mol^{-1}; k_{0i} in h^{-1}; β in h^{-1})

Hydrolysis substrate	Kinetic parameters	Model	
		B	D
Xylan	ln k_{0F}	50.2	50.2
	E_{aF}	188	188
	ln k_{0S}	19.9	–
	E_{aS}	125	–
	α	0.916	0.916
	δ	8.49	8.49
Xylooligomers	ln k_{2max}	50.5	50.7
	E_{a2}	167	150
	β	$1.36 \cdot 10^{-6}$	$5.82 \cdot 10^{-6}$
	δ	15.83	17.18
Xylose	ln k_{03}	21.7	21.6
	E_{a3}	69.0	69.0
	δ	15.09	17.25

This reaction scheme corresponds to Model 2 in Fig. 3, which has been successfully employed for the kinetic modelling of Eucalyptus wood autohydrolysis under isothermal[9] or non-isothermal[11] conditions.

Kinetic Modelling of Araban and Acetyl Group Autohydrolysis

Chemical composition of the hemicellulosic fraction of rice husks corresponds to acetylated arabinoxylan. In this polymer, the corresponding constituents (arabinose, xylose and acetyl groups) are present in the

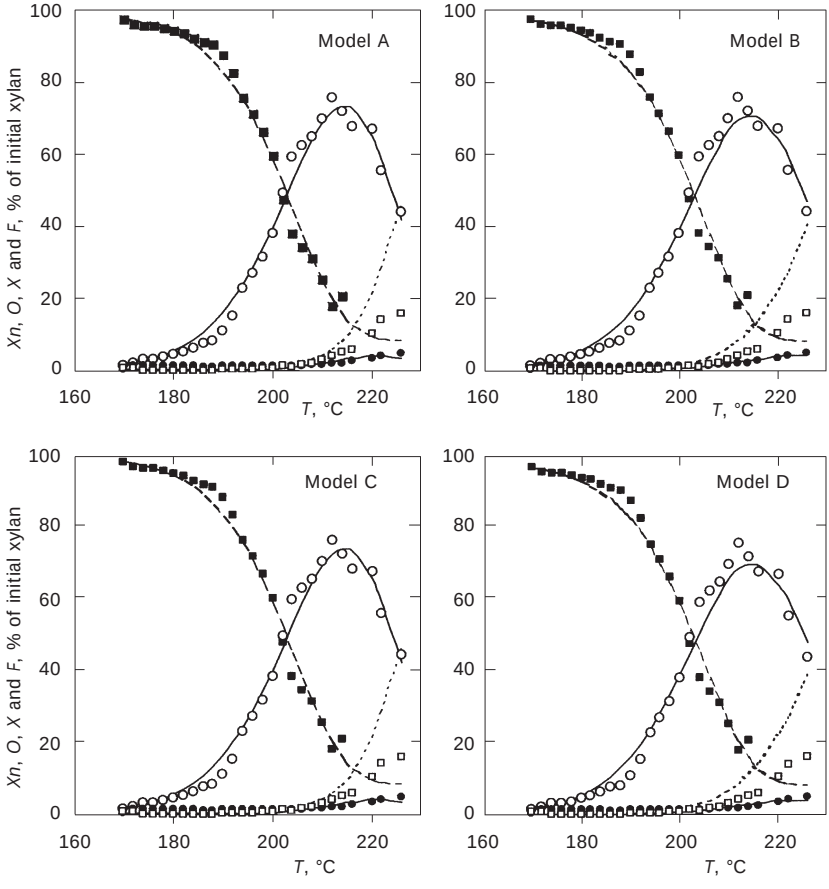

FIG. 6

Experimental values of variables *Xn* (exp. ■, calc. – – –), *O* (exp. ❍, calc. ——), *X* (exp. ●, calc. ——) and *F* (exp. ❑, calc. · · · ·), and results calculated for the same variables using the models A to D

proportions shown in Table I. From these results, it can be calculated that the molar ratio xylose : arabinose is about 9 : 1, whereas the molar ratio acetyl groups : pentoses is 0.29 : 1.

For calculation purposes, the araban degradation was considered to proceed independently of xylan hydrolysis. The analytical data allow to distinguish between arabinose units (or acetyl groups) remaining in the solid phase as a polymer, arabinose units (or acetyl groups) solubilised as oligomers and free arabinose (or free acetic acid).

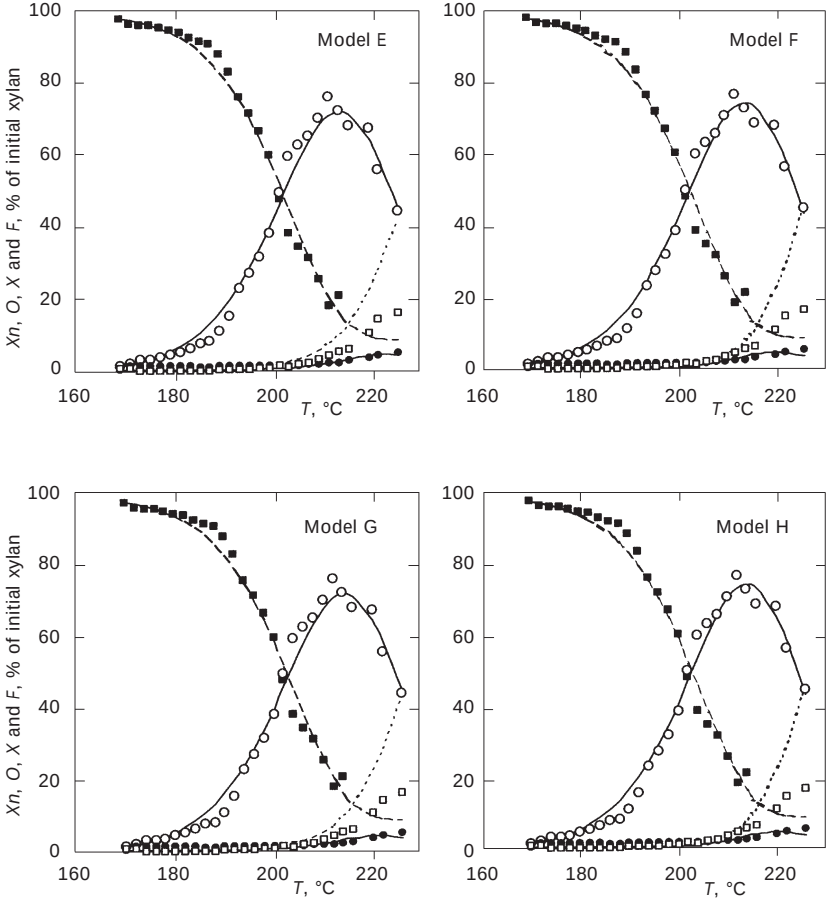

FIG. 7

Experimental values of variables *Xn* (exp. ■, calc. – – –), *O* (exp. ❍, calc. ——), *X* (exp. ●, calc. ——) and *F* (exp. ❑, calc. · · · ·), and results calculated for the same variables using the models E to H

Experimental data concerning the autohydrolyis of araban and acetyl groups are shown in Fig. 8. As expected, araban was more susceptible to autohydrolysis than xylan, as proved by comparison of temperatures leading to maximum concentrations of arabinose oligomers (204 °C) and xylan oligomers (212 °C). An intermediate behaviour was observed for acetyl groups (the maximum concentration of acetyl groups linked to oligomers was reached at 210 °C). The high reactivity of araban was confirmed by the high conversion of arabinooligomers to arabinose under the most severe reaction conditions considered (50%, in comparison with 5% xylooligomer conversion to xylose under the same conditions). The decrease in arabinose concentration observed at the end of the reaction confirms the participation of parasitic reactions leading to sugar consumption in the overall reaction scheme.

Based on the above findings, the simplest reaction scheme allowing a satisfactory interpretation of araban degradation is similar to Model C in Table II

$$Arn_F \xrightarrow{k_1} Arn_O \xrightarrow{k_2} Ar \xrightarrow{k_3} \text{degradation products},$$

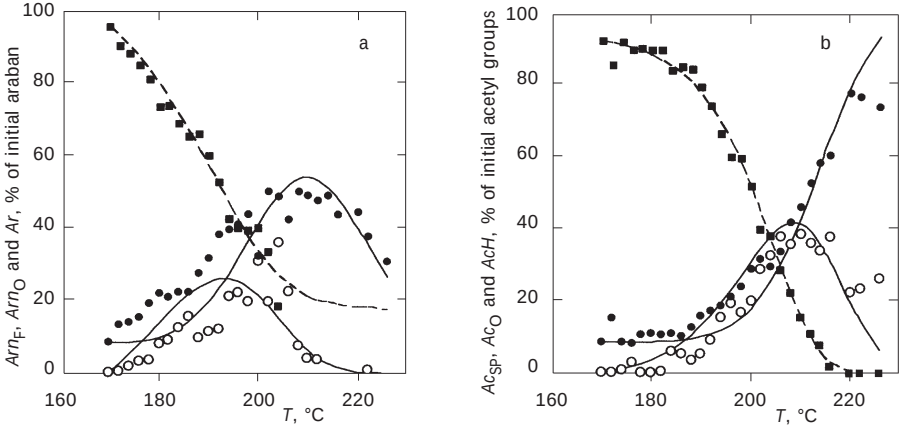

FIG. 8

Experimental values of araban variables Arn_F, Arn_O and Ar, and results calculated for the same variables using model C (a). Experimental values of acetyl groups variables Ac_{SP}, Ac_O and AcH, and results calculated for the same variables using model C (b). Polymers (exp. ■, calc. – – –), oligomers (exp. ❍, calc. ——) and monomers (exp. ●, calc. ——)

where Arn_F denotes the fast-reacting araban, Arn_O stands for arabinose oligomers and *Ar* for arabinose. The fitting of data led to the results listed in Table V, which allowed the calculation of the corresponding concentration profiles (see Fig. 8a). The increased deviations of experimental from calculated results in comparison with the case of xylan autohydrolysis are caused by a comparatively low araban content in the feedstock.

The interpretation of acetyl group hydrolysis was carried out using a closely related mechanism, in which the consumption of acetic acid was neglected, in accord with a simplification of model C ($k_3 = 0$)

$$Ac_{SP} \xrightarrow{k_1} Ac_O \xrightarrow{k_2} AcH$$

where Ac_{SP} denotes the percentage of acetyl groups linked to the solid phase (*i.e.*, to the unreacted xylan or araban), Ac_O corresponds to the acetyl groups linked to oligomers, and *AcH* corresponds to the free acetic acid. Table V includes the results obtained by data fitting, and Fig. 8b confirms the fair interpretation of the experimental behaviour provided by this approach.

TABLE V
Values calculated for the kinetic parameters participating in the hydrolytic degradation of araban and acetyl groups (E_{ai} in kJ mol^{-1}; k_{0i} in h^{-1})

Hydrolysis substrate	Kinetic parameters	Araban	Acetyl groups
Polymers	ln k_{0F}	35.9	53.2
	E_{aF}	129	200
	α	0.750	1.00
	δ	10.1	7.99
Oligomers	ln k_{02}	34	30.8
	E_{a2}	121	113
	δ	52.6	36.0
Monomers	ln k_{03}	27	–
	E_{a3}	101	–
	δ	47.2	–

CONCLUSIONS

The non-isothermal autohydrolysis of rice husk hemicelluloses (acetylated arabinoxylan) was assessed by experiments which allowed the determination of concentration profiles of unreacted substrates and reaction products (sugar oligomers, sugars, furfural, furfural decomposition products and acetic acid). The behaviour of the system was modelled by means of first-order pseudohomogenous kinetics. Eight different kinetic models (based on consecutive and parallel reactions) were tested to describe the xylan decomposition, and the whole set of kinetic parameters involved in each model was calculated. The related mechanisms gave a close interpretation of the hydrolysis of araban and acetyl groups. The models proposed for degradation of the various fractions making part of the hemicellulosic fraction of rice husks provide the basic information necessary for design and economic evaluation of autohydrolysis, the treatment that can be conceived as the first step of a multistage fractionation process leading to full utilisation of the feedstock.

SYMBOLS

AcH	weight percentage of initial acetyl groups converted into acetic acid
Ac	percentage of initial acetyl groups linked to the considered fraction
Ar	weight percentage of initial araban converted to arabinose
Arn	initial weight percentage of araban in samples
E_a	activation energy, kJ mol^{-1}
F	weight percentage of initial xylan converted to furfural
k	kinetic coefficient, h^{-1}
k_0	pre-exponential factor, h^{-1}
n	number of measurements
O	weight percentage of initial xylan converted to xylooligomers,
R	universal gas constant, 8.314 J mol^{-1} K^{-1}
T	absolute temperature, K
X	weight percentage of initial xylan converted to xylose
Xn	weight percentage of initial xylan contained in samples
α	susceptible fraction in initial xylan, kg kg^{-1}
β	empirical parameter for the time dependence of rate constants, h^{-1}
δ	mean relative quadratic deviation (percentage)
τ	time, h

Subscripts

0	initial
calc	calculated values of variable
exp	experimental values of variable
F	fast fraction

max	maximum value
O	oligomers
S	slow fraction
SP	concerning the solid phase

REFERENCES

1. Myerly R. C., Nicholson M. D., Katzen R., Taylor J. M.: *CHEMTECH* **1981**, *11*, 186.
2. Maloney M. T., Chapman T. W., Baker A. J.: *Biotechnol. Bioeng.* **1985**, *27*, 355.
3. Bouchard J., Nguyen T. S., Chornet E., Overend R. P.: *Bioresour. Technol.* **1991**, *36*, 121.
4. Aoyama M., Seki K.: *Holz als Roh- und Werkstoff* **1994**, *52*, 388.
5. Aoyama M., Seki K., Saito, N.: *Holzforschung* **1995**, *49*, 193.
6. Saska M., Ozer E.: *Biotechnol. Bioeng.* **1995**, *45*, 517.
7. Shimizu K., Sudo K., Ono H., Ishihara M., Fujii T., Hishiyama S.: *Biomass Bioenergy* **1998**, *14*, 195.
8. Conner A. H., Lorenz L. F.: *Wood Fiber Sci.* **1986**, *18*, 248.
9. Garrote G., Domínguez H., Parajó J. C.: *J. Chem. Technol. Biotechnol.* **1999**, *74*, 1101.
10. Garrote G., Domínguez H., Parajó J. C.: *Process Biochem. (Oxford)* **2001**, *36*, 571.
11. Garrote G., Domínguez H., Parajó J. C.: *J. Food Eng.* **2002**, *52*, 211.
12. Ichikawa T., Mitsumura Y.: *Nippon Kasei Gakkaishi* **1996**, *47*, 445; *Chem. Abstr.* CAN 371753 1996.
13. Imaizumi K., Nakatsu Y., Sato M., Sedarnawati Y., Sugano M.: *Agric. Biol. Chem.* **1991**, *55*, 199.
14. May T., Mackie R. I., Garleb K. A.: *Mikrooekol. Ther.* **1995**, *23*, 158.
15. Campbell J. M., Fahey J. C., Wolf B. W.: *J. Nutr.* **1997**, *127*, 130.
16. Okazaki M., Fujikawa S., Matsumoto N.: *Bifidobacteria Microflora* **1990**, *9*, 77.
17. Okazaki M., Koda H., Izumi R., Fujikawa S., Matsumoto N.: *J. Jpn. Soc. Nutr. Food Sci.* **1991**, *44*, 41.
18. Garrote G., Domínguez H., Parajó J. C.: *Bioresour. Technol.* **2001**, *79*, 155.
19. Browning B. L.: *Methods of Wood Chemistry*. John Wiley & Sons, New York 1967.
20. Parajó J. C., Alonso J. L., Santos V.: *Ind. Eng. Chem. Res.* **1995**, *34*, 4333.
21. Carrasco F., Roy C.: *Wood Sci. Technol.* **1992**, *26*, 189.
22. Kobayashi T., Sakai Y.: *Bull. Agric. Chem. Soc. Jpn.* **1956**, *20*, 1.
23. Conner A. H.: *Wood Fiber Sci.* **1984**, *16*, 268.
24. Carrasco F., Chornet E., Overend R. P., Heitz M.: *Can. J. Chem. Eng.* **1987**, *65*, 71.
25. Abatzoglou N., Chornet E., Belkacemi K., Overend R. P.: *Chem. Eng. Sci.* **1992**, *47*, 1109.
26. Jacobsen S. E., Wyman C. E.: *Appl. Biochem. Biotechnol.* **2000**, *84–86*, 81.
27. Abatzoglou N., Koeberle P. G., Chornet E., Overend R. P., Koukios E. G.: *Can. J. Chem. Eng.* **1990**, *68*, 627.
28. Maloney M. T., Chapman T. W., Baker A. J.: *Biotechnol. Prog.* **1986**, *2*, 192.
29. Saeman J. F.: *Ind. Eng. Chem.* **1945**, *37*, 43.
30. Goldstein I. S. in: *Wood and Agricultural Residues*, p. 315. Academic Press, Inc. 1983.
31. Abatzoglou N., Bouchard J., Chornet E., Overend R. P.: *Can. J. Chem. Eng.* **1986**, *64*, 781.
32. McKibbins S. W., Harris J. F., Saeman J. F., Neill W. K.: *Forest Prod. J.* **1962**, *19*, 17.
33. Mok W. S.-L., Antal M. J., Varhegyi G.: *Ind. Eng. Chem. Res.* **1992**, *31*, 94.

34. Harris J. F., Baker A. J., Conner A. H., Jeffries T. W., Minor J. L., Pettersen R. C., Scott R. W., Springer E. L., Wegner T. H., Zerbe J. I.: *Gen. Tech. Rep. FPL-45*. Forest Product Laboratory, Madison 1985.
35. Bouchard J., Abatzoglou N., Chornet E., Overend R. P.: *Wood Sci. Technol.* **1989**, *23*, 343.
36. Madeleine J. L., Bouvier J. M., Gelus M.: *Wood Sci. Technol.* **1990**, *24*, 143.
37. Parajó J. C., Vázquez D., Alonso J. L., Santos V.: *Holz als Roh- und Werkstoff* **1993**, *51*, 357.
38. Kim S. B., Lee Y. Y.: *Biotechnol. Bioeng. Symp.* **1987**, *17*, 71.
39. Brennan A., Hoagland W., Schell D. J.: *Biotechnol. Bioeng. Symp.* **1986**, *17*, 53.
40. Mehlberg T., Tsao G. T.: Presented at *178th ACS National Meeting, Washington D. C., 1979*.